RESEARCH ARTICLE

Crawling without wiggling: muscular mechanisms and kinematics of rectilinear locomotion in boa constrictors

Steven J. Newman and Bruce C. Jayne*

ABSTRACT

A central issue for understanding locomotion of vertebrates is how muscle activity and movements of their segmented axial structures are coordinated, and snakes have a longitudinal uniformity of body segments and diverse locomotor behaviors that are well suited for studying the neural control of rhythmic axial movements. Unlike all other major modes of snake locomotion, rectilinear locomotion does not involve axial bending, and the mechanisms of propulsion and modulating speed are not well understood. We integrated electromyograms and kinematics of boa constrictors to test Lissmann's decades-old hypotheses of activity of the costocutaneous superior (CCS) and inferior (CCI) muscles and the intrinsic cutaneous interscutalis (IS) muscle during rectilinear locomotion. The CCI was active during static contact with the ground as it shortened and pulled the axial skeleton forward relative to both the ventral skin and the ground during the propulsive phase. The CCS was active during sliding contact with the ground as it shortened and pulled the skin forward relative to both the skeleton and the ground during the recovery phase. The IS shortened the ventral skin, and subsequent isometric activity kept the skin stiff and shortened during most of static contact while overlapping extensively with CCI activity. The concentric activity of the CCI and CCS supported Lissmann's predictions. Contrary to Lissmann, the IS had prolonged isometric activity, and the time when it shortened was not consistent with providing propulsive force. Decoupling propulsion from axial bending in rectilinear locomotion may have facilitated economical locomotion of early snakes in subterranean tunnels.

KEY WORDS: Snake, Muscle, Electromyography, Movement, Skin

INTRODUCTION

The different body plans of animals have profound consequences for how and where animals are able to move, and elongate, limbless bodies occur in diverse animal phyla such as Annelida, Nematoda and Chordata and have evolved independently several times. Many of the most common types of limbless animal locomotion bend the long axis of the animal and propagate bends posteriorly to provide propulsive forces for both aquatic and terrestrial movement (Gray, 1968; Alexander, 2003). In taxa such as vertebrates with segmented body plans, the evolution of elongate and limbless forms has occurred by increasing the number of body segments rather than elongating individual body segments. Consequently, an important general issue for understanding the neural control of movement is how such animals coordinate the muscle activity and movement among all of these serially homologous structures. Within vertebrates, both lampreys and snakes have body segments with size and shape that are relatively uniform along most of their length, and the absence of appendages provides a somewhat simplified body plan that makes both of these groups well suited for studying the neural control of rhythmic axial movements (Cohen, 1988). Furthermore, snakes use different modes of locomotion in a variety of environments, which facilitates investigating the diversity and plasticity of axial motor patterns.

Most previous studies recognize at least four major modes of terrestrial snake locomotion (Mosauer, 1932; Gray, 1968; Gans, 1974; Jayne, 1986; Cundall, 1987), but rectilinear is the only one of these that does not use axial bending to generate propulsive forces (Lissmann, 1950). The different types of snake locomotion with axial bending have been identified for many decades, and their muscular mechanisms are known (Jayne, 1988b,c; Gasc et al., 1989; Moon and Gans, 1998). Nearly 70 years ago, a classic study with boa constrictors (Lissmann, 1950) qualitatively described the movements involved in rectilinear locomotion and hypothesized patterns of muscle activity. However, aside from one additional kinematic and modeling study of rectilinear locomotion (Marvi et al., 2013), few advances have been made.

During rectilinear locomotion of snakes, the skin moves relative to the skeleton (Lissmann, 1950). Detailed anatomical descriptions of the muscles presumed relevant for these movements have long been known (Buffa, 1904), but experimental data on their activity have been lacking. Snakes have some specialized (costocutaneous) muscles that extend from the ribs to the ventral and ventrolateral regions of the skin (Fig. 1). The fibers of the costocutaneous superior (CCS) and costocutaneous inferior (CCI) muscles extend posteriorly and anteriorly, respectively, from their origins on a rib and the longitudinally oriented fibers of the interscutalis muscle (IS) extend between adjacent ventral scales (Fig. 1). The ventral and ventrolateral skin of snakes has both lower stiffness (Jayne, 1988a) and more mobility relative to the skeleton than the skin in the mid-dorsal region, which is firmly attached to the neural spines of the vertebrae.

Much of Lissmann's synthesis of the kinematics of rectilinear locomotion leading to hypothesized muscle activity was presented graphically (Lissmann, 1950, fig. 7). We relied mainly on Lissmann's classic figure (Fig. 2A) to summarize his hypotheses of how muscle activity was related to skin movement, but some details not apparent in the figure were obtained from his verbal descriptions. During rectilinear locomotion, the mid-dorsal skin of the snake has a constant length and progresses forward with a nearly constant speed relative to the ground (Fig. 2A). By contrast, the ventral skin has variable length as it oscillates longitudinally relative to the mid-dorsal region and alternately has sliding and static contact with the ground (Fig. 2A,B). If the CCS, CCI and IS muscles were all activated as their fibers shortened, as proposed by Lissmann, then the pattern of activity would be as illustrated in Fig. 2B.

Department of Biological Sciences, PO Box 210006, University of Cincinnati, Cincinnati, OH 45221-0006, USA.

*Author for correspondence (bruce.jayne@uc.edu)

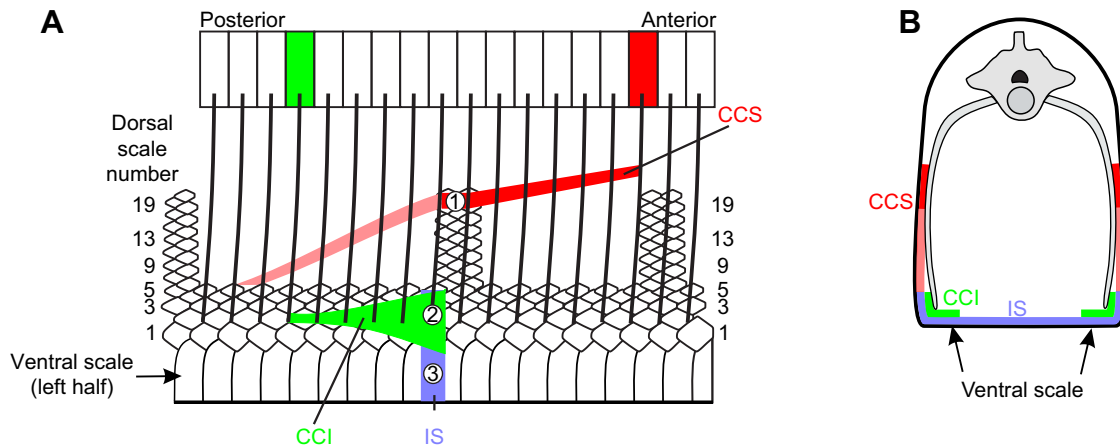S.J.N., 0000-0002-5127-3143; B.C.J., 0000-0003-2564-7524

Fig. 1. Schematic views of muscles from which electromyograms (EMGs) were obtained. Red, green and blue indicate the costocutaneous superior (CCS), costocutaneous inferior (CCI) and interscutalis (IS) muscles, respectively. The lighter shade of red indicates the less mobile portion of the CCS, for which the fibers were firmly connected to the skin along their entire length. (A) Internal view of the left side of the snake. The thick oblique lines indicate ribs. The rectangles represent vertebrae, for which red and green indicate the vertebrae of origin for the CCS and CCI, respectively, acting on a single longitudinal location. Unlike for the intact snake, the ventral skin was peeled back into a parasagittal plane so that the mid-ventral line is at the bottom of the figure. White circles indicate approximate electrode positions for the CCS (1), CCI (2) and IS (3). Muscle segments are only shown with insertions on the same longitudinal segment of the skin. The numbers on either side of the figure indicate the scale row number, which is counted from ventral to dorsal. (B) Cross-section. The anterior portion of the CCI overlaps and is dorsal to the underlying fibers of the IS. The entire width of the ventral scale and the first two dorsal scale rows on both sides of the snake usually contact the ground.

We quantified the kinematics and muscle activity of rectilinear locomotion to test the following previously proposed hypotheses (Lissmann, 1950; Fig. 2B, Table 1). The CCS, CCI and IS should all be active only while their fibers shorten (concentric activity). The CCS and CCI are functional antagonists with no overlap in activity. The IS is the primary propulsor muscle. Table 1 summarizes more detailed expectations for the timing of muscle activity. We also compared axial motor patterns, mechanisms for modulating speed and the mechanisms of propulsion during rectilinear locomotion with diverse types of locomotion with some analogous mechanical demands.

MATERIALS AND METHODS
Experimental subjects
We used seven captive-bred boa constrictors, *Boa constrictor* Linnaeus 1758. However, we only quantitatively analyzed the

Table 1. Lissmann's hypotheses for muscle activity and our experimental results for rectilinear locomotion

Lissmann (1950) prediction	Our study
CCI onset immediately after CCS offset	Yes
CCI onset at beginning of static contact	Yes
CCI onset between times 4 & 5 (Fig. 2)	No
CCI activity throughout static contact	Yes
CCI propulsive function	Yes
CCS onset immediately after CCI offset	No
CCS onset between times 2 & 3 (Fig. 2)	No
CCS onset at beginning of sliding	No
CCS offset between times 4 & 5 (Fig. 2)	Yes
CCS antagonist to CCI	Yes
CCS no overlap with CCI	Yes
CCS recovery phase function	Yes
IS onset at beginning of skin shortening	No
IS shortens skin	Yes
IS activity only while skin shortens	No
IS propulsive function	No

CCI, costocutaneous muscle; CCS, costocutaneous muscle; IS, interscutalis muscle (Fig. 1).

results from the four individuals in which electrodes remained in place for all three non-homologous muscles of interest at a single longitudinal location. These four individuals had similar overall sizes as indicated by snout–vent length (mean SVL=118 cm, range=113–125 cm), total length (mean=132 cm, range=127–138 cm) and mass (mean=916 g, range=808–1017 g). The number of pre-cloacal vertebrae ranged from 235 to 244 and had a mean value of 240. We maintained all snakes in cages with incandescent light bulbs that allowed them to thermoregulate their daytime body temperatures from 25 to 33°C, and the body temperatures of snakes during all experiments were between 29 and 31°C, which is within the range of field active body temperatures for this species (Montgomery and Rand, 1978).

To facilitate quantifying the motion of the snake skin, we attached reflective markers to the skin at two longitudinal locations that were an average of nine vertebrae apart (Figs 3A, 4A). The surface of all markers was reflective tape (Scotchlite 7610 reflective tape, 3M, St Paul, MN, USA). The mid-dorsal markers were reflective spheres with a diameter of 9.5 mm (B&L Engineering, Santa Ana, CA, USA), whereas all other markers were disks of tape with a diameter of 2.5 mm. All research was conducted in compliance with the Institutional Animal Care and Use Committee of the University of Cincinnati (protocol no. 07-01-08-01).

Experimental apparatus
We performed preliminary experiments to determine what materials elicited rectilinear locomotion and allowed us to record the relevant movements. The overall horizontal surface of the test apparatus was 362 cm long and 46 cm wide. Snakes commonly follow the edges of surfaces, and we wanted the snakes to be straight. Consequently, to guide the movements of the snakes, we added a vertical wall, 46 cm high, that extended the length of the overall surface, and to prevent glare from this background, we covered it with gray gaffers tape (P-655, Shurtape, Hickory, NC, USA) in the working section of the apparatus (Fig. 3A). Mid-way along the length of the overall surface (Fig. 3A), we covered a rectangular hole 99×36 cm with a piece of UV non-glare acrylic sheet (Acrylite, Evonik Corp., Parsippany, NJ, USA), so that we
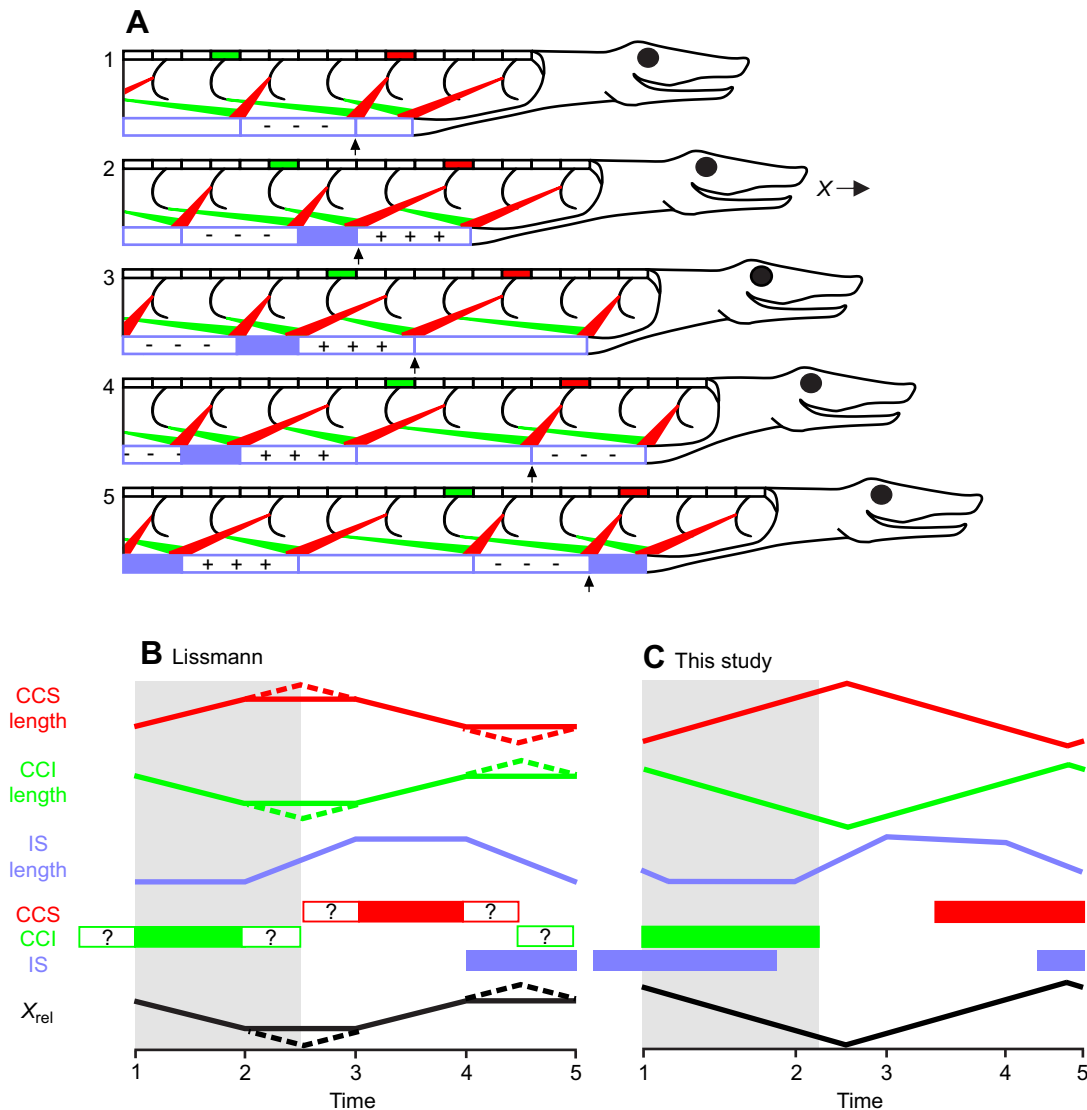
Fig. 2. Events during one cycle of rectilinear locomotion. In A–C, red, green and blue indicate locations of or events associated with the costocutaneous superior (CCS), costocutaneous inferior (CCI) and interscutalis (IS) muscles, respectively. (A) A modified illustration of the model of Lissmann (1950, fig. 7). Note that not all vertebrae and ribs are shown in this schematic diagram. The ventrally located fill patterns of solid blue, +, white and − indicate maximally shortened, lengthening, maximally lengthened, and shortening of the ventral skin, respectively. The black arrows indicate the ventral location of interest for data in B, and the colored rectangles indicate the skeletal segments that give rise to the relevant CCS (red) and CCI (green) muscles. The numbered events for the ventral skin (=IS length) were as follows: (1) beginning of static contact (or cessation of forward movement when slipping occurred), (2) beginning of lengthening, (3) end of lengthening, (4) beginning of (rapid) shortening, and (5) beginning of static contact. The lengths of the costocutaneous muscles are proportional to the distance between the reference vertebrae (colored rectangle) and focal ventral scale (arrow). Note that the position of the ventral skin oscillates longitudinally relative to the underlying skeleton and mid-dorsal skin (X_{rel}). In B and C, time intervals shaded gray indicate static contact between the ventral skin of the snake and the surface. (B) Schematic graphical summary of hypothesized muscle activity (colored horizontal bars) and changes in muscle length based on Lissmann (1950, fig. 7). The solid lines are based only on the events shown in A (and Lissmann, 1950, fig. 7), whereas the dashed lines integrate information from verbal descriptions. Decreasing values for the black line showing X_{rel} indicate that the ventral skin is being retracted (moved posteriorly to the mid-dorsal region). The colored fills within the horizontal bars denoting hypothesized muscle activity are based on activity only during fiber shortening (based on A), whereas the open portions of the rectangle containing question marks indicate possible times of muscle activity based on the verbal descriptions. (C) Working model of events during rectilinear locomotion based on experiments of the present study. The average times of muscle activity are based on their relationships to static contact. To simplify the diagram in C and facilitate comparisons with Lissmann, some nuances were not taken into account. For example, the different dorsoventral locations of the insertions of the CCI and CCS cause different amounts and rates of shortening of the CCI versus the CCS that are not shown.

could record movements of the ventral skin. To reduce the amount of slipping on the acrylic sheet, every 2 cm along the length of the apparatus we placed 2×48 mm strips of clear packing tape (Scotch, 3M) that was 0.05 mm thick. The acrylic sheet was surrounded by artificial turf (Greenline Synthetic Artificial Lawn Turf, Greenline, Austin, TX, USA) so that the top of the acrylic sheet was flush with the top of the artificial turf (Fig. 3A). Having the two surfaces flush to each

other greatly reduced the tendency of the snakes to perform lateral undulation by pushing against the edge where these two materials met. To provide a distance scale, we used an indelible marker to draw reference lines on both the vertical and horizontal surfaces (Fig. 3A).

The apparatus we used was usually effective for obtaining rectilinear locomotion. However, we were not able to control the speed of the animals because stimulating snakes to move often
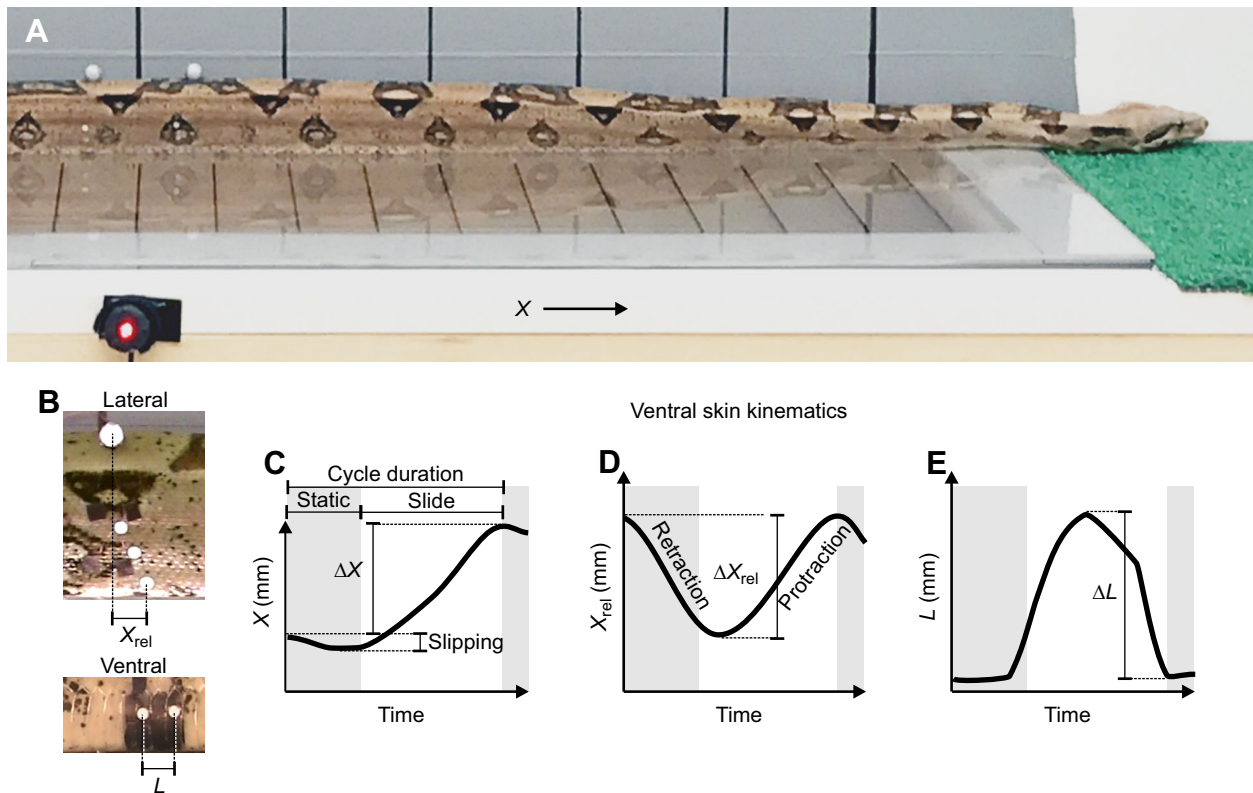
Fig. 3. Experimental apparatus and kinematic methods. (A) A *Boa constrictor* performing rectilinear locomotion on our apparatus. The red LED was used to synchronize kinematic and EMG data. (B) Close up of reflective markers used to track skin movements. (C) Forward movement of the ventral skin maker relative to the ground. (D) Movement of the ventrolateral skin relative to the mid-dorsal marker (vertebra). (E) Change in the length (*L*) of the ventral skin. Note that C–E have different scales for their *y*-axes.

caused them to flex their bodies or perform lateral undulation rather than rectilinear locomotion. Consequently, we did not attempt to elicit maximal speed.

Kinematics

We obtained high-definition (1920×1080 pixels) video images at a rate of 60 Hz for both lateral and ventral views. Both cameras were perpendicular to the long axis of the experimental surface. We placed LEDs within view of both cameras (Fig. 3A), and the 1 s square-wave voltage that activated the LED was sent to one of the channels of the analog-to-digital converter that collected all electromyographic data. Hence, the lateral and ventral videos and the electromyograms (EMGs) could be synchronized to within 17 ms of each other.

We used the auto-tracking feature of Maxtraq software (Innovision Systems, Inc., Columbiaville, MI, USA) to perform frame-by-frame analysis of movement, and the *x*-axis of our coordinate system was parallel to the long axis of the experimental apparatus (Fig. 3A). We analyzed eight cycles of movement per individual, for which EMGs of all desired muscles were present. We digitized the two-dimensional coordinates of the reflective markers at the mid-dorsal location (MD), and the third and eighteenth dorsal scale rows (Figs 3B, 4A). The third dorsal scale row was the most ventral dorsal scale row that was consistently visible in lateral view because the first two dorsal scale rows and the ventral scales all touched the ground (Figs 1B, 3B). To determine the position (Fig. 3C), length (*L*) and change in length per cycle (Δ*L*) (Fig. 3E) of the ventral skin, we digitized the coordinates of markers on ventral scutes that were two scales apart (Fig. 3B). Preliminary experiments established that auto-tracking of markers and the accuracy of skin length changes were better when the markers were two ventral scales apart rather than on adjacent ventral scales.

We calculated eight additional kinematic variables from the coordinates of the reflective markers (Fig. 5). For the ventral marker with a longitudinal location closest to the lateral markers, we determined two successive times at the beginning of static contact to determine the duration of the kinematic cycle (Fig. 3C). We then calculated the frequency of movement by inverting cycle duration (Fig. 5A). We determined the forward distance that a ventral scale marker (Δ*X*) traveled per cycle relative to a fixed reference point on the ground (Figs 3C, 5C). The average forward velocity was Δ*X* divided by cycle duration (converted to % SVL s^{-1}). We expressed the duration of static contact as a percentage of the cycle duration, duty factor (Figs 3C, 5E). We used 'static contact' to refer to the cessation of forward movement of the ventral skin relative to the supporting surface. However, a small amount (approximately 2 mm) of backward slipping often did occur (Fig. 4E), and we quantified the amount of this per cycle (Figs 3C, 5G) by taking the difference between the *x*-coordinates at the beginning and end of where the *x*-coordinate of the ventral scale marker had a negative slope (Fig. 3C). The mid-dorsal skin attaches firmly to the vertebrae and was used as a proxy for vertebral movements. The *x*-coordinate of the mid-dorsal marker was also used as a relative frame of reference to determine the longitudinal location (*X*$_{rel}$) of other landmarks as they oscillated relative to the underlying skeleton (Fig. 3B), and we subsequently calculated the total change in relative longitudinal position per cycle for various landmarks (Δ*X*$_{rel}$) (Figs 3D, 5D).
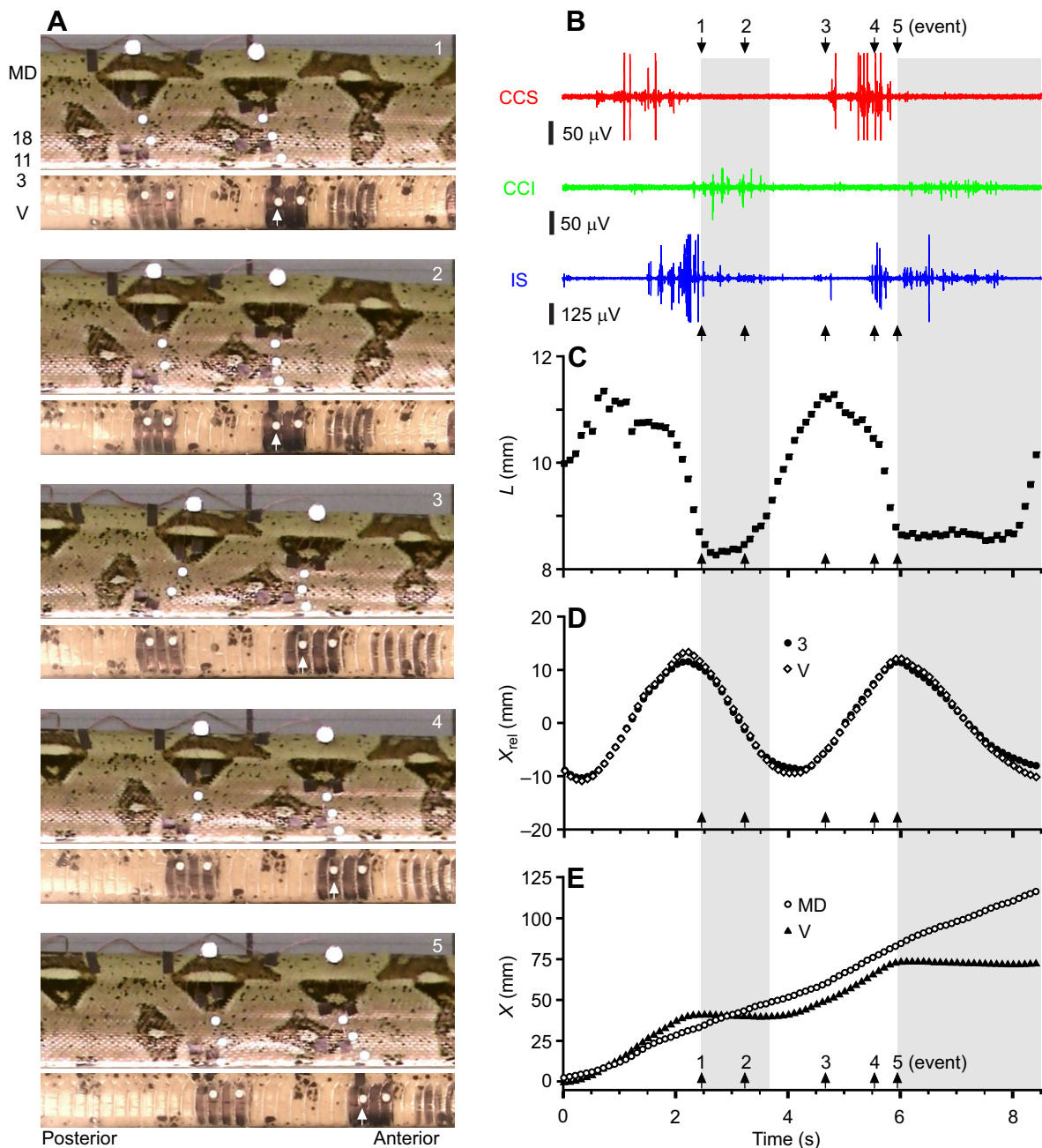
Fig. 4. Synchronized images of skin movement, kinematics and muscle activity during rectilinear locomotion. (A) Video images for one cycle of motion showing views of the right side (top) and ventral scales (bottom). The white arrows indicate the longitudinal location for the data shown in B–E at the following events: (1) beginning of ventral static contact, (2) beginning of ventral skin lengthening, (3) end of ventral skin lengthening, (4) beginning of rapid shortening of the ventral skin and (5) beginning of ventral static contact of the ventral scale as shown in Fig. 2. The conventions for naming the lateral view landmarks are to the left of the first panel. MD, mid-dorsal; V, ventral. (B–E) Muscle activity and movement during two cycles of rectilinear locomotion. Black arrows indicate the times of the corresponding video images shown in A. (B) EMGs. Red, green and blue indicate the costocutaneous superior (CCS), costocutaneous inferior (CCI) and interscutalis (IS) muscles, respectively. (C) Length of the skin between adjacent markers on the ventral scales within a longitudinal site (A, white arrows). (D) Longitudinal displacement of markers on the ventral scale (black fill) and 3rd dorsal scale row (white fill), relative to the mid-dorsal marker at the same site. (E) Longitudinal displacement of the ventral scale (black fill) and mid-dorsal marker (white fill) relative to the supporting surface. The gray regions indicate when the belly was in static contact with the substrate (see Movie 1).

We estimated strains of the muscles as follows. For the CCS, we only considered the anterior, highly mobile portion that spans approximately six body segments (Fig. 1A). We determined the resting lengths of the costocutaneous muscles from dissections of preserved specimens in a mid-body region where the body was straight, and for both the CCI and CCS this length was approximately 30 mm. We assumed that both the CCI and the CCS had a longitudinal orientation of fibers whose changing lengths would be detected by the changing values of X_{rel}. We also assumed that equal amounts of shortening and lengthening occurred within each of these muscles within one cycle; hence, we used one-half ΔX_{rel} as the change in length from rest. We then divided one-half ΔX_{rel} by resting length and expressed the result as a percentage. Using similar assumptions for the IS muscle, we
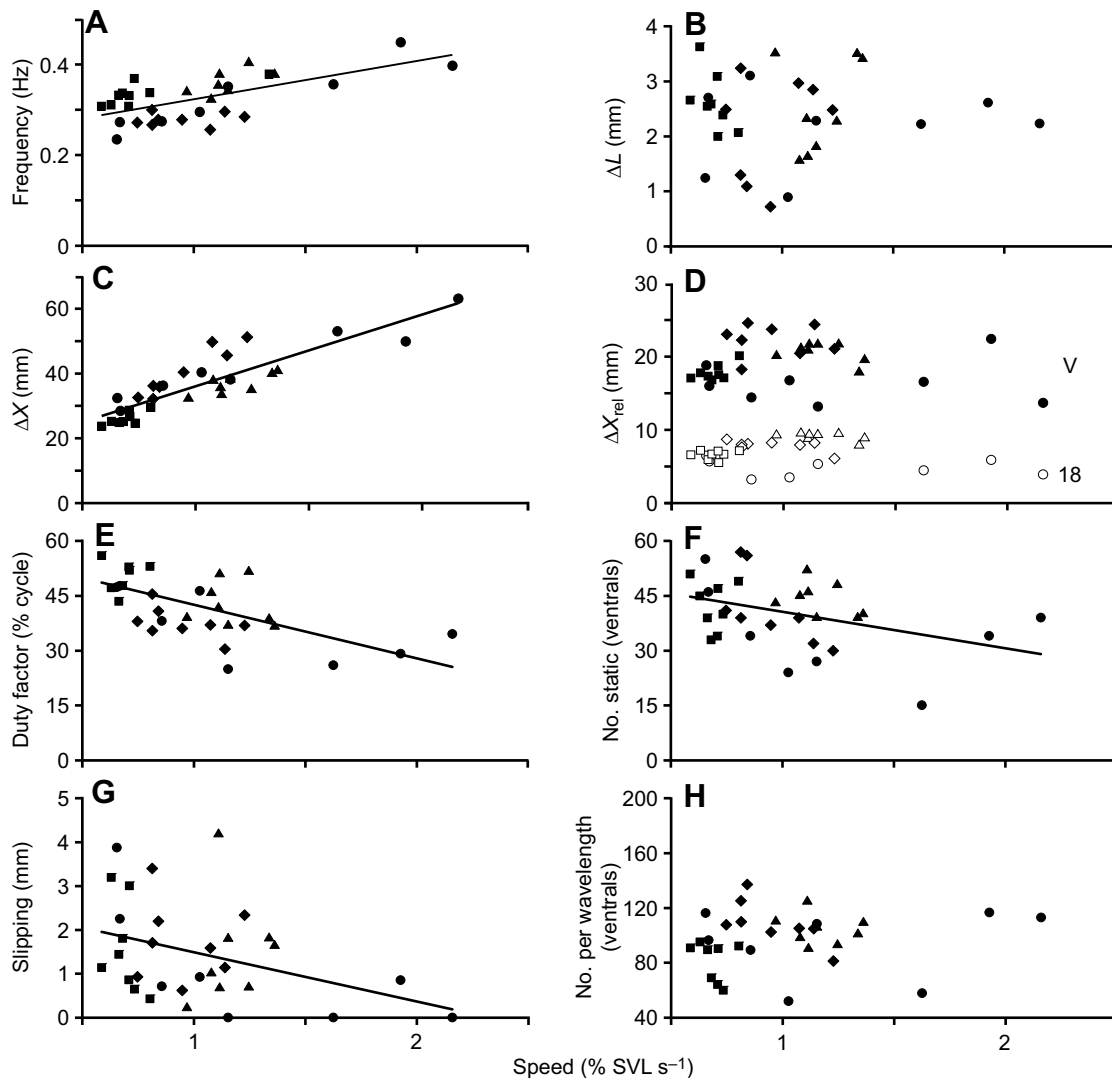
Fig. 5. Effects of speed on kinematic variables. Regression lines are only shown for significant relationships (see Table 2 for significant regression statistics). In each panel, N=32 and the four different symbol shapes indicate the four individuals from which the data were obtained. (A) Frequency. (B) Change in ventral skin length (ΔL) per cycle (R^2=0.001, P=0.8). (C) Forward displacement (ΔX) per cycle of the ventral scale relative to a fixed point of reference. (D) Longitudinal displacement (ΔX_{rel}) of the ventral scale (black fill) (R^2<0.01, P=0.95) and dorsal scale row 18 (white fill) (R^2=0.01, P=0.58) relative to the mid-dorsal scale row and during static contact of the ventral scale. (E) Duty factor. (F) Number of ventral scales simultaneously in static contact per cycle. (G) Backwards slipping per cycle. (H) Number of ventral scales per anatomical wavelength (R^2<0.01, P=0.95).

estimated muscle strain as one-half of ΔL (Fig. 3E) divided by the mean value of L.

We also directly determined the number of adjacent ventral scales with simultaneous static contact (Fig. 5F) that were anterior to the ventral scale of interest at the first moment it established static contact. An anatomical wavelength includes the two regions with all of the adjacent scales that are in either static or sliding contact, but this involved so many body segments it could rarely be determined directly. Consequently, we multiplied the number of ventral scales in static contact by the duration of the entire cycle divided by the duty factor to estimate the anatomical wavelength (Fig. 5H).

Electromyography

We made bipolar EMG electrodes using 0.05 mm-diameter, poly-coated stainless steel wire (California Fine Wire, Grover City, CA, USA) that was approximately 3 m long, and we followed general methods of electrode construction detailed previously (Jayne, 1988b). We inserted the electrodes percutaneously using 26-guage hypodermic

needles, and rather than using anesthesia, we used gentle manual restraint during this procedure. We secured the wires to the skin using small pieces of black gaffers tape (6910 Gaffers tape, 3M).

We implanted electrodes at two longitudinal sites near mid-body that were 8–10 vertebrae apart. At each site, we implanted five electrodes, attempting to locate two electrodes in both the CCS and the CCI and one electrode in the IS such that electrodes in the three non-homologous muscles would be in muscle segments acting on the same longitudinal location within the skin of the snake (Fig. 1A). After successful experiments, we killed the animals with an overdose of anesthetic (sodium pentobarbital) and performed post-mortem dissections to verify the electrode locations.

We obtained analog EMGs using Grass P511 pre-amplifiers (Grass Instruments Co., Quincy, MA, USA) with high-pass and low-pass filters with cut-off frequencies of 30 Hz and 10 kHz, respectively, as well as a 60 Hz notch filter. We converted the analog EMGs to digital data using a PowerLab 16SP and LabChart software (AD Instruments, Colorado Springs, CO, USA) with a

sampling frequency of 4 kHz and a digital high-pass filter with a cut-off frequency of 50 Hz. We used the LabChart software to manually quantify the onsets and offsets of EMGs.

Data analysis

We converted the absolute times of EMG onsets and offsets to relative times that were a percentage of a cycle. To facilitate meaningful pooling and analyzing of EMG data across all trials, we then made corrections for the variable proportion of static contact within each cycle. For example, if static contact ended at 40% within one cycle and at 80% of another cycle and if an EMG offset occurred at the midpoint of static contact, then the uncorrected relative times of EMG offset would be 20% and 40% of a cycle, respectively. However, after correcting for the variable proportions of static contact, both relative times of EMG offset would be 30% after the beginning of a standardized cycle with a mean proportion of static contact that was 60% of a cycle. The mean duration of static contact for all trials (N=32) that was used as the standardized cycle for our data was 42% of a cycle.

For the relative times of EMGs, we used mixed-model ANOVA (Systat 13, Systat Software, Inc., San Jose, CA, USA) where muscle (N=3) was a fixed, crossed factor and individual (N=4) was a random, crossed factor. We nested cycle (N=8) within individual as a random factor to account for repeated observations of EMGs among non-homologous muscles within each cycle. We also used Tukey's procedure to test which relative times differed significantly from each other. To determine whether kinematic variables changed significantly with increased speed, we performed least-squares regressions. For all analyses, we used a significance level of $P<0.05$, and all mean values are reported ±s.e.m.

RESULTS
Anatomy
The following descriptions of the musculature of *Boa constrictor* were based on the average measurements from the four individuals that we used for our quantitative analysis. Two (costocutaneous) muscles extended from the ribs to the skin in opposite directions. The fibers of the CCS muscle originated from the rib approximately one-third the distance from its head to its tip and extended posteriorly for approximately six body segments before initially inserting onto dorsal scale rows 16–18 (Fig. 1A). The fibers in the anterior portion of the CCS segment (Fig. 1A, dark red) were highly mobile and only surrounded by very diffuse connective tissue, and we obtained EMGs from the posterior portion of this highly mobile part of the CCS (Fig. 1A). By contrast, the additional fibers of the CCS that were posterior to the initial attachment site (Fig. 1A, light red) were firmly attached to the skin along their entire length and had

a more ventral orientation as they extended nearly to the fifth dorsal scale row (Fig. 1A). Fibers from the CCI muscle originated near the tip of the rib, and they extended anteriorly for approximately six body segments before fanning out and attaching to the skin from dorsal scale row five to the lateral portion of the ventral scale (Fig. 1A). The fibers of the CCI were dorsal (and deep) to all of the more superficial intrinsic cutaneous muscles (Fig. 1B). Boa constrictors have several muscles intrinsic to the skin (Buffa, 1904), but we only obtained EMGs from the cutaneous muscle whose fiber orientation seemed most likely to shorten the skin longitudinally. The IS muscle (the interscuto-squamali of Buffa, 1904) had longitudinally oriented fibers that crossed the hinge region between two adjacent ventral scales (Fig. 1A). Some fibers of the IS also extended for one body segment along dorsal scale rows 1–5, and the most medial fibers of an IS from one side were located along the mid-ventral line of the belly of the snake (Fig. 1; Buffa, 1904). The IS was the most superficial intrinsic cutaneous muscle in the ventral portion of the snake that contacted the ground. Some other more obliquely oriented intrinsic cutaneous muscles, that were not the subject of our study, form additional deeper layers that were between the IS and CCI (Buffa, 1904).

Kinematics
The forward speeds observed for rectilinear locomotion were quite slow and ranged from 0.6 to 2.2% SVL s^{-1} (7–26 mm s^{-1}), and speed had widespread effects on kinematics (Fig. 5). As speed increased, significant increases (Table 2) occurred in both frequency of movements (Fig. 5A) and the forward movement per cycle (Fig. 5B), whereas significant decreases (Table 2) occurred in duty factor (Fig. 5E), the number of ventral scales with simultaneous static contact (Fig. 5F), and the amount of slipping per cycle (Fig. 5G). In a few cases, no slipping was observed (Fig. 5G), and even at the slowest speed, when the predicted amount of slipping was greatest (2.0 mm), this was only 7% of ΔX.

Speed did not significantly affect ΔL, ΔX_{rel} and anatomical wavelength. The mean value of ΔL (two ventral scales apart) was 2.3±0.14 mm, and ΔL ranged from approximately 1 to 3 mm (Fig. 5B), and this mean value corresponded to a strain for the IS and ventral skin of ±12%. Hence, considerable stretching of the skin occurred ventrally. The amplitudes of ΔX_{rel} increased from dorsal to ventral (Figs 4A, 5D) as the mean values for scale rows 18 and 3 and the ventral scale were 7.1±0.3, 17.1±0.5 and 19.1±0.5 mm, respectively, all of which differed significantly from each other (paired t-tests, $P<0.001$). The anatomical wavelength (Fig. 5H) had a mean value of 96±3.6 ventral scales.

At a given longitudinal site, the longitudinal oscillations of landmarks relative to the mid-dorsal mark were in phase with each

Table 2. Least-squares regressions for kinematic variables as a function of speed (% SVL s^{-1})

Dependent variable	Coefficients +95% CL		R^2 (P)	Predicted values	
	Slope	Intercept		0.6% SVL s^{-1}	2.2% SVL s^{-1}
Frequency (Hz)	0.084±0.038	0.24±0.04	0.41 (<0.001)	0.29	0.42
ΔX (mm)	22.0±4.5	14.3±4.8	0.77 (<0.001)	27.5	62.7
Duty factor (% cycle)	−10.8±7.0	51.4±7.6	0.25 (0.004)	45	28
Static ventrals	−9.76±8.56	50.3±9.2	0.15 (0.027)	44	29
Slipping (mm)	−1.13±1.04	2.62±1.13	0.14 (0.035)	1.94	0.13
Ventral retraction speed (% SVL s^{-1})	0.75±0.26	0.05±0.34	0.54 (<0.001)	0.50	1.71

N=32 for all regressions. Frequency: the inverse of cycle duration (Fig. 3C); ΔX: forward distance traveled per cycle (Fig. 3D); duty factor: duration of static contact divided by cycle duration (Fig. 3C); static ventrals: number of adjacent ventral scales with simultaneous static contact; slipping: backward movement of marked ventral scale per cycle (Fig. 3C); ventral retraction: average speed of posterior movement of the skin relative to the vertebrae=ΔX_{rel} divided by time taken to move posteriorly (Fig. 3D). SVL, snout–vent length; CL, confidence limit.

other (Fig. 4A,D). For example, the timing of the maximal values of ΔX_{rel} did not differ significantly between the ventral scale and dorsal scale row 3 (paired t=0.6, P=0.3). Consequently, points along the side of the snake that formed a vertical line at rest created an oblique line oriented anterioventrally at the beginning of static contact and posterioventrally shortly after static contact (Fig. 4A).

Between different longitudinal sites, the longitudinal oscillations of the skin relative to the mid-dorsal mark were out of phase with each other as a result of the posterior propagation of events (Fig. 4A, image 4; Fig. 6B). Dividing the number of vertebrae between the two longitudinal locations by the lag time between maximal values of the longitudinal position of scale row 3 (X_{rel3}) at the two locations yielded an average speed of posterior propagation of 32± 5.0 vertebrae s^{-1}.

The following movements occurred during one cycle. The ventral skin periodically had static contact with the ground (Fig. 4A,E), whereas the mid-dorsal region moved forward with a nearly constant velocity (Fig. 4E). During most of static contact, the ventral skin remained maximally shortened (Fig. 4C). Occasionally, when a focal ventral scale had static contact, some shortening of the ventral skin occurred (Fig. 4C, near 2.5 s) as the adjacent more-posterior ventral scale was pulled forward towards the focal scale. Near the end of static contact, some lengthening of the ventral skin occurred as it was stretched anterior to the focal scale with static contact (Fig. 4C, near 3.7 s). Large and rapid amounts of ventral skin shortening usually occurred slightly before the initiation of static

contact (Fig. 4C, near 6 s), and this was often preceded by a rather slow and minimal amount of shortening (Fig. 4C, 4.7–5.5 s). On average, 90% of the total amount of shortening was during rapid shortening. Most of the rapid lengthening of the skin usually occurred during the first half of sliding contact (Fig. 4C, 3.7–4.7s).

Muscle activity

Activity of the CCI and CCS usually occurred during static and sliding contact, respectively (Fig. 4B). Hence, we did not observe any substantial overlap of activity in these two anatomical antagonists. By contrast, the IS was active both during late sliding contact and during most of static contact; hence, its activity overlapped that of both the CCS and the CCI (Fig. 4B).

For the standardized (% cycle duration) onset times of the CCI and IS and the offset times of the CCS (Fig. 7A), an ANOVA revealed a highly significant effect of muscle ($F_{2,6}$=15.9, P=0.004) as a result of the onset of the IS activity occurring significantly before both the onset of the CCI (Tukey HSD=10.4%, P<0.001) and the offset of the CCS (Tukey HSD=8.5%, P<0.001). The 95% confidence limits of both the offset time of the CCS and the onset of the CCI encompassed the start of static contact (Fig. 7A, 0% of a

Fig. 7. Mean timing of muscle activity relative to kinematic events. The mean values were from data pooled across all individuals and trials (N=32). The left and right edges of the colored horizontal bars indicate EMG onset and offset, respectively, and the thick black horizontal lines indicate s.e.m. (A) EMGs relative to static and sliding contact. The mean duration of static contact is 42% of a cycle. (B) EMGs relative to longitudinal movements of scale row 3 (X_{rel3}) relative to the mid-dorsal location. The transition between posterior and anterior movement occurred at a mean value of 49% of a cycle. (C) EMGs relative to the events involved in ventral skin length. The vertical lines at 0%, 19%, 48% and 74% of a cycle indicate the beginning of: rapid shortening (RS), maximally shortened (MS), lengthening (L) and slow shortening (SS), respectively.
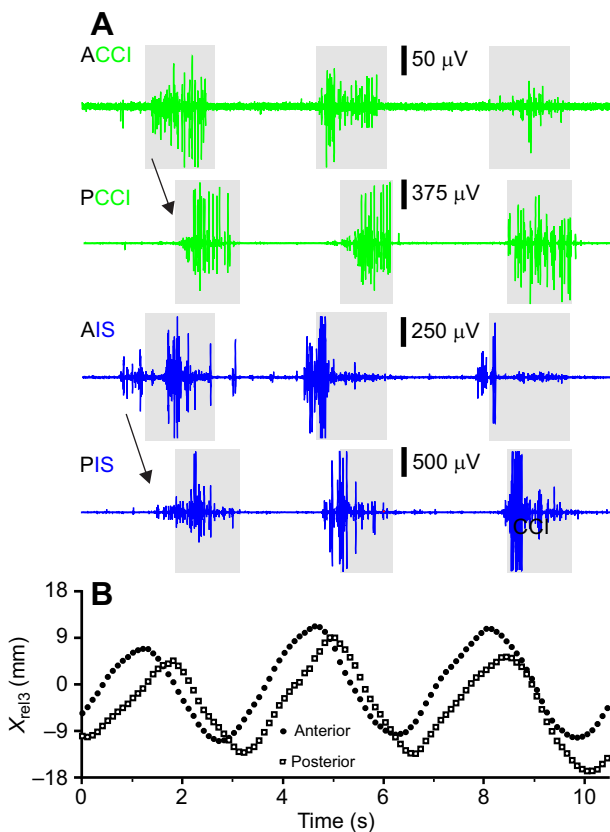

Fig. 6. Posterior propagation of muscle activity and kinematics. (A) EMGs from the costocutaneous inferior (CCI, green) and interscutalis (IS, blue) muscles from anterior (A) and posterior (P) sites that were 10 vertebrae apart. (B) Longitudinal position of scale row 3 (X_{rel3}) relative to the mid-dorsal marker for the anterior (black fill) and posterior (white fill) sites. Note that the events of the posterior site lagged behind those of the anterior site.
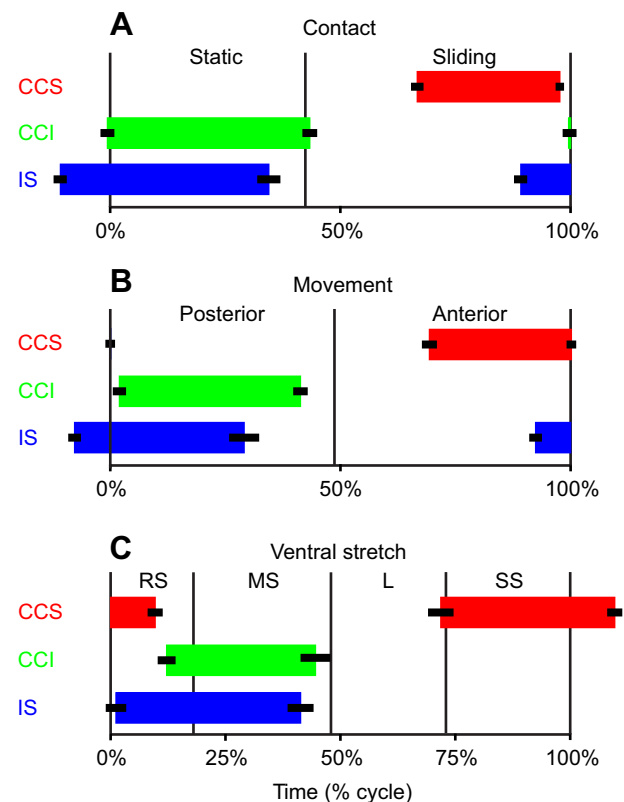
cycle). By contrast, the onset of IS activity preceded the start of static contact by 11% of a cycle (Fig. 7A).

For the standardized offset times of the CCI and IS and the onset times of the CCS (Fig. 7A), the effect of muscle was highly significant ($F_{2,6}$=12.7, P=0.007), and all of the pair-wise comparisons of these three events were significantly different from each other (Tukey HSD, all $P<0.001$). The 95% confidence limits of the mean relative offset time of the CCI (43%) encompassed the start of sliding contact (Fig. 7A, 42% of a cycle). The mean relative offset of the IS (34%) was well within the static contact portion of the cycle, whereas the mean onset time of the CCS (67%) was well within the sliding contact portion of the cycle (Fig. 7A).

Fig. 7B shows the standardized times of muscle activity based on the longitudinal movements of the dorsal scale row 3 relative to mid-dorsal region, for which the duration of the skin moving posteriorly averaged 48.7±0.86% of a cycle. CCS activity occurred mainly as the skin moved anteriorly (protraction), with mean onset and offset times of 69.3±1.6% and 99.9±1.1%, respectively. By contrast, CCI activity occurred mainly when the skin moved posteriorly (retraction), with mean onset and offset times of 2.2±1.5% and 41.3±1.6%, respectively. The activity of the IS preceded that of the CCI as the mean times of onset and offset of the IS were −7.8±1.4% and 29.1±3.3% of a cycle, respectively.

We also standardized EMG onsets and offsets relative to the time intervals during: (1) rapid shortening (mean duration=18.0±0.05% of a cycle), (2) maximally shortened (29.9±0.08%), (3) lengthening (25.0±0.05%) and (4) slow-shortening/lengthened plateau of ventral skin length (27.0+0.03%) (Fig. 7C). Effectively no activity of the CCS, CCI and IS occurred as the ventrolateral skin lengthened (Fig. 7C, 48–73%). The mean onset time of the CCS (71.9±2.8%) nearly coincided with the beginning of slow shortening of the ventral skin, and the offset of activity occurred roughly mid-way during rapid shortening of the skin (9.1±1.7%) (Fig. 7C). Most activity of the CCI occurred while the skin remained maximally shortened (mean onset=12.2±2.0%, mean offset=44.6± 3.3%) (Fig. 7C). The mean onset of IS activity nearly coincided with the beginning of rapid shortening of the skin (1.2±1.8%) and activity continued for a substantial time after the skin had been maximally shortened (mean offset=41.3±2.8%).

Similar to the kinematic events for different longitudinal locations, the timing of muscle activity of the posterior site lagged behind that of the more anterior site (Fig. 6). Consequently, muscle activity was propagated posteriorly. We could not directly calculate the mean speeds of EMG propagation for all trials because we were not always successful in obtaining EMGs from serially homologous muscles at both of the longitudinal sites within every individual.

DISCUSSION
Comparisons with Lissmann's model
Our kinematic data were consistent with the experimental findings of Lissmann (1950) (Figs 1, 3, 4 and 5). However, Lissmann (1950) (Fig. 3) did observe a greater average relative amount of backwards slipping (14±1.6% ΔX) compared with our study (4.5±0.7% ΔX).

Overall, Lissmann (1950) hypothesized that the CCS, CCI and IS muscles were active as their fibers shortened (Fig. 2B), but some of his statements and graphical summaries were not always unambiguous and consistent (e.g. Table 1, rows 2 and 3). For example, Lissmann's graphical model by itself suggests periods without a length change in the CCS and CCI (Fig. 2A,B, times 2–3 and 4–5). This is probably just a result of a limited number of illustrations per unit time. Both Lissmann (1950) and our study

documented continuous oscillations of the ventral skin relative to the mid-dorsal locations (Fig. 2B,C), which imply continuously changing lengths of the CCS and CCI. Some statements that an event occurred 'between' two times could indicate either the midpoint (assumed in Fig. 2B) or anywhere within a time interval.

Overall, our findings support Lissmann's suggestions that both the CCS and CCI are active as their fibers shorten. The CCI and CCS are also antagonists with activity in the propulsive and a recovery phase, respectively (Table 1). A propulsive function of the CCI muscle is implied by its activity throughout static contact as the skeleton slid forward relative to both the ventral skin and the ground (Figs 4 and 7). We also observed some lengthening of the ventral skin that occurred without any clearly associated muscle activity. This supports Lissmann's suggestion that some stretching of the ventral skin occurs passively, perhaps from more anterior muscular events with forces that are transmitted through tension in the skin or inactive muscle fibers.

The lack of a direct propulsive role of IS during its shortening and its subsequent isometric activity are two key differences between our findings and Lissmann's hypotheses (Table 1). Initial IS activity did occur as the ventral skin shortened (concentric activity), but subsequent isometric IS activity occurred while the skin remained maximally shortened (Figs 2C and 7C). The initial slow shortening of the ventral skin before onset of IS activity (Figs 2C, 4 and 7C) probably resulted from CCS activity, and the subsequent combined activity of the CCS and IS could have increased the rate of shortening. Lissmann also suggested that shortening of the IS provided the primary propulsive force for rectilinear locomotion. However, the only way this shortening within the skin could contribute to propulsion is if a mechanical linkage were present to transmit force to the underlying skeleton. The CCI seems to be the only logical mechanical linkage for this function, but the IS activity during ventral skin shortening occurred without CCI activity (Fig. 4). Consequently, the shortening of the ventral skin by itself seems unlikely to directly propel the skeleton forward. Later, when activity of the IS did overlap with that of the CCI, the skin was maximally shortened and not changing length (Fig. 4, 6–8 s).

Mechanisms for modulating speed
With increased speed, limbed animals commonly use different gaits, and the percentage of a cycle for the propulsive phase of a given limb (duty factor) decreases (Hildebrand, 1976). Diverse animals also commonly change speed by some combination of modulating the frequency or amplitude of movements. Consequently, the locomotion of snakes has many parallels with the locomotion of other animals as they commonly change the type of locomotion with increased speed and use frequency and amplitude modulation to vary the speed within a particular type of locomotion. For example, stride frequency, stride length and step length of limbed animals are analogous to the frequency of skin oscillations (Fig. 5A), ΔX (Fig. 5C) and ΔX_{rel} for the ventral scale (Fig. 5D), respectively, for the rectilinear locomotion in our study.

Compared with other modes of terrestrial snake locomotion, rectilinear locomotion is quite slow, and if we stimulated the boa constrictors too much, they used modes with axial bending such as lateral undulation and concertina locomotion. The range of speeds that we observed (0.6–2.2% SVL s^{-1}) for rectilinear locomotion encompassed the range of speeds reported collectively (0.6–1.6% SVL s^{-1}) in two previous studies (Lissmann, 1950; Marvi et al., 2013). Speeds reported for the terrestrial lateral undulation of some colubrid snakes (SVL <100 cm) can range from

approximately 20 to 200% SVL s^{-1} (Jayne, 1986; Jayne and Bennett, 1990). The speeds of concertina locomotion may range from 2 to 29% SVL s^{-1} depending on the species and tunnel width (Jayne and Davis, 1991). No previous experiments with rectilinear locomotion attempted to elicit maximal speeds, and the speeds at which snakes change from rectilinear locomotion to another mode remain unknown. However, we know of no species of snake that attains maximal speed using rectilinear locomotion.

In light of the large ranges of speed among and within different modes of locomotion, it is interesting to consider what changes with speed. Unlike our study, Lissmann (1950) did not quantify the effects of speed, and most of the variation in speed reported in Marvi et al. (2013) occurred between different species and snakes with large differences in overall size. However, we found that several kinematic variables including frequency, 'stride length' (ΔX) and duty factor changed significantly with speed of rectilinear locomotion (Table 2). Unexpectedly, none of the amplitudes of skin movement per cycle (Fig. 5B,D) changed significantly with speed. Consequently, the primary mechanisms for modulating the speed of locomotion appear to be increasing the frequency of movements and the speed of skin retraction by decreasing the time during which nearly constant amplitudes of skin retraction occur. The most relevant skin movement for propulsion seems to be the retraction of the ventral skin relative to the skeleton during static contact, and these values of speed predicted from a regression with snake speed had a 3.3-fold increase that corresponded closely with the 3.6-fold variation in the forward speeds of the snakes in our study (Table 2).

Comparisons of axial motor patterns

The locomotion of diverse elongate and limbless animals with segmented body plans commonly involves motor patterns that are propagated posteriorly (Cohen, 1988) as occurs during the swimming of fishes and salamanders (Williams et al., 1989; Frolich and Biewener, 1992) and all but one of the modes of snake locomotion that involve axial bending (Jayne, 1988c). Hence, the posteriorly propagated stimulus that is also in the motor pattern of rectilinear locomotion seems likely to reflect the retention of a very old vertebrate trait.

For propagated motor patterns, the number of adjacent serial homologs with simultaneous muscle activity is the product of the speed of propagation (in segments per unit time) times the EMG duration. These quantities for the muscles during the rectilinear locomotion of boa constrictors (Fig. 6) indicate that more than 30 adjacent body segments often have simultaneous muscle activity. Rather than ending activity of one axial muscle segment before activating the next more posterior segment, a recurrent finding for axial motor patterns of phylogenetically diverse vertebrates is that several adjacent serial homologs are simultaneously active (Williams et al., 1989; Frolich and Biewener, 1992; Jorgensen and Jayne, 2017). Rectilinear locomotion resembles all of the propagated epaxial motor patterns of snakes (Jorgensen and Jayne, 2017) because the number of adjacent muscle segments with simultaneous activity usually exceeds the number of body segments spanned by an individual muscle segment (Fig 1A). Consequently, in snakes and many other vertebrates, all of the contractile tissue from all of the axial muscle segments that overlap a particular skeletal segment commonly have substantial amounts of time with simultaneous activity.

Additional general features of motor patterns used for propulsion via axial bending are that at a particular longitudinal location, muscle segments are only active on one side (unilateral) as activity alternates rhythmically between the left and right sides (Jayne, 1988b; Williams et al., 1989; Frolich and Biewener, 1992). Hence, muscles with the antagonistic functions of flexing the animal to the right or left lack overlapping activity. We did not record EMGs on both sides of the boa constrictors, but the synchronous movement of the skin on the left and right sides implies bilateral muscle activity. Additionally, muscles with the antagonistic functions of protracting (CCS) and retracting (CCI) the skin lacked overlapping activity. Unilateral activity during the locomotion of fishes and salamanders suggests that the presence of unilateral activity of the epaxial muscles during snake locomotion (Jayne, 1988b) is probably a trait that was retained from a very distant ancestor of snakes, and reciprocal inhibition is a common feature of the spinal circuits of vertebrates (Cangiano and Grillner, 2005). By contrast, the occurrences of bilateral activity during rectilinear locomotion and in the epaxial muscles of snakes when they lift or support their body above the ground (Jayne, 1988c; Jorgensen and Jayne, 2017) seem likely to be evolutionary novelties that have arisen independently within snakes. Although some of the epaxial muscles of snakes may be activated either unilaterally or bilaterally, it remains unclear whether this is also the case for the costocutaneous and cutaneous muscles of snakes. Perhaps this latter issue could be tested by having snakes perform rectilinear locomotion with a sharp turn to one side.

Functions of skin and muscle

During rectilinear locomotion, snakes use their skin rather than bone to transmit propulsive forces. This is unusual for a vertebrate and poses some intriguing problems. For example, decreased stiffness of the skin facilitates its movement relative to the skeleton during rectilinear locomotion as well as the expansion needed for consuming large prey whole. By contrast, low skin stiffness is ill-suited for transmitting propulsive forces. However, the isometric activity of the IS during static contact was consistent with preventing the ventral skin from being stretched posteriorly while transmitting force to the ground as the CCI pulled the skeleton forward relative to the ventral skin and the ground. Hence, the snakes used muscle activity to modulate the stiffness of the skin in a manner that is reminiscent of how swimming fishes commonly use increasing amounts of eccentric muscle activity to increase flexural stiffness of the posterior vertebral column (Tytell et al., 2010). Furthermore, the more dorsal skin of snakes is stiffer (Jayne, 1988a) where cutaneous muscles are absent and cannot modulate skin stiffness.

The lack of a skeletal lever-arm system for the propulsive muscles of rectilinear locomotion is also unusual for a vertebrate. Hence, the speeds of locomotion for such a 'direct drive' system should be constrained rather directly by the strains and strain rates of the relevant muscles, which have a nearly longitudinal orientation of their fibers (Fig. 1). When we integrated our kinematic and anatomical data for rectilinear locomotion, we obtained mean estimates of *in vivo* muscle strain of ±12%, ±32% and ±12% for the IS, CCI and CCS, respectively. Given that most vertebrate muscles usually experience *in vivo* strains less than ±20% of rest length (Burkholder and Lieber, 2001), the estimated strain of the CCI is quite high.

Swallowing large prey could also affect the strain and locomotor function of the costocutaneous muscles because of the attendant increase in the distance between the tips of the ribs and the ventral scales (Cundall and Greene, 2000). Although it may not be as extreme as the 200% strain reported for the circumferentially oriented fibers of the intermandibularis muscle of snakes during swallowing (Close et al., 2014), nonetheless, the costocutaneous

muscles may experience much larger strains after swallowing a large meal. After consuming large meals, many snakes also appear to have an impeded ability to flex the vertebral column (Crotty and Jayne, 2015), which suggests another possible benefit for being able to perform rectilinear locomotion.

Many heavy-bodied species of snakes such as vipers and terrestrial boas and pythons seem particularly adept at performing rectilinear locomotion, and some of these taxa are also noteworthy for the large meals that they consume (Pough and Groves, 1983). A rarely considered functional consequence of the relatively short tails in many of these same taxa is that a larger fraction of their entire length can contribute to propulsion during rectilinear locomotion. Furthermore, some of the stout bodied vipers also have only about one-half the number of pre-cloacal vertebrae of many boas and pythons. Consequently, if the CCI muscles span the same number of body segments when the number of vertebrae varies for snakes with equal SVL, then the CCI muscle could produce greater absolute amounts of shortening for a given amount of muscle strain in vipers. This, in turn, may permit faster absolute speeds of muscle shortening and enhance the locomotor speeds of rectilinear locomotion of species with fewer vertebrae.

Some of the patterns of movements and mechanical events involved in rectilinear locomotion have mechanical analogs with other taxa and types of locomotion. For example, because of the alternating pattern of static and sliding contact in rectilinear locomotion, comparisons with the concertina locomotion of snakes and earthworm locomotion are common (Lissmann, 1950; Marvi et al., 2013). Entire body segments stop completely both for earthworm locomotion (Gray and Lissmann, 1938; Quillin, 1999) and during concertina locomotion, and the resulting large changes in momentum are probably a key factor contributing to a higher energetic cost of concertina locomotion compared with other types of terrestrial snake locomotion (Walton et al., 1990; Secor et al., 1992). By contrast, during the rectilinear locomotion of snakes, only the integument periodically has static contact with the ground as all other structures move forward continuously. The small mass of snake skin compared with that of the rest of the body suggests a large amount of forward momentum is conserved during rectilinear locomotion, which could reduce its energetic cost.

Earthworms are one of the few groups of elongate, limbless animals other than snakes that can crawl with a straight body, and their locomotor muscles also lack rigid lever arms to amplify their contractile speed, which resembles rectilinear locomotion of snakes (Gray and Lissmann, 1938; Quillin, 1999). Unlike the muscles used during rectilinear locomotion, the fibers of the primary propulsors for earthworms are perpendicular to: (1) the long axis of the body, (2) the overall direction of movement, and (3) the muscles with antagonistic function. The elongation speeds of muscular hydrostats can exceed the speed of contraction of the circumferential fibers when cylinders are long compared with their diameter (Kier and Smith, 1985). By contrast, the CCI muscles of snakes appear to lack any mechanism for amplifying their speed of contraction.

Similar to rectilinear locomotion, the locomotion of earthworms is slow (1–10% total length s^{-1}), and increased speed of earthworms is correlated with increased forward distance traveled per cycle, increased frequency of movement and decreased duty factor (Quillin, 1999). Earthworms also use increased amplitude of protrusion movements as an important mechanism for increasing speed, whereas the rectilinear locomotion of boa constrictors relies mostly on increased frequency and increased speed of movement to increase speed. Snakes performing concertina locomotion in narrow tunnels also rely mainly on modulating frequency rather than the amplitude of movements to increase speed (Jayne and Davis, 1991). Perhaps the spatial constraints of fitting into confined spaces reduces the ability of animals with rigid skeletons to modulate the amplitudes of their movement to increase speed.

The skin during rectilinear locomotion and the body segments during earthworm locomotion also both have distinct propulsive and recovery phases. Rather than contributing to propulsion, recovery phase movements only reposition a structure so that a subsequent movement can contribute to propulsion. Distinct propulsive and recovery phases are also universal for the terrestrial locomotion of limbed animals, but for snake locomotion, they only occur for two of four modes of terrestrial locomotion: concertina (Jayne, 1986) and rectilinear. Potentially, the existence of a recovery phase could be detrimental to attaining high speeds as any one structure with a recovery phase is not generating propulsive forces for a significant amount of time. However, having many propulsive structures such as limbs or the serially homologous structures in snakes (and earthworms) reduces this problem, as some structures can contribute to propulsion while other structures are being repositioned. During rectilinear locomotion, this simultaneous use of serial homologs clearly occurs as more than 100 ventral scales may simultaneously have static contact as the CCI muscles pull the snake forward.

A potential benefit of both rectilinear locomotion and the peristaltic locomotion of earthworms is allowing locomotion with a straight body in spaces as small as the cross-sectional area of the animal. Snakes performing rectilinear locomotion have a remarkably constant external shape and cross-sectional area. This constancy of external shape exceeds that of: (1) limbed locomotion, (2) limbless locomotion that uses axial bending and (3) earthworm locomotion, which involves changing both the length and diameter of body segments.

Snakes are a monophyletic group that probably evolved from burrowing ancestors (Yi and Norell, 2015), for which an ability to move in form-fitting spaces was probably important. Costocutaneous muscles occur not only in all extant snakes but also in a clade of nearly 200 species of amphisbaenians that are limbless and specialized burrowers (Gans, 1974). This is a striking example of convergent evolution as snakes and amphisbaenians do not form a monophyletic group (Pyron et al., 2013) and costocutaneous muscles are absent in other squamate reptiles. Concertina locomotion in tunnels is the energetically most demanding mode of snake locomotion that involves bending, and it becomes even more demanding as tunnel width decreases (Walton et al., 1990; Jayne and Davis, 1991). Consequently, interactions between the spatial constraints of underground movement and energetic economy probably contributed to independent origins of morphological and behavioral specializations that allow limbless animals to crawl without wiggling. Subsequently, when speed is not at a premium, many species of snakes also may rely on rectilinear locomotion even when they move above ground.

Supplementary information

Supplementary information available online at
http://jeb.biologists.org/lookup/doi/10.1242/jeb.166199.supplemental

References

Alexander, R. M. (2003). *Principles of Animal Locomotion*. Princeton, NJ: Princeton University Press.

Buffa, P. (1904). Ricerche sulla muscolatura cutanea dei serpenti e considerazioni sulla locomozione di questi animali. *Atti della Accademia scientifica veneto-trentino-istriana* **1**, 145-237.

Burkholder, T. J. and Lieber, R. L. (2001). Sarcomere length operating range of vertebrate muscles during movement. *J. Exp. Biol.* **204**, 1529-1536.

Cangiano, L. and Grillner, S. (2005). Mechanisms of rhythm generation in a spinal locomotor network deprived of crossed connections: the lamprey hemicord. *J. Neurosci.* **25**, 923-935.

Close, M., Perni, S., Franzini-Armstrong, C. and Cundall, D. (2014). Highly extensible skeletal muscle in snakes. *J. Exp. Biol.* **217**, 2445-2448.

Cohen, A. H. (1988). Evolution of the vertebrate central pattern generator for locomotion. In *Neural Control of Rhythmic Movements in Vertebrates* (ed. A. H. Cohen. S. Rossignol and S. Grillner), pp. 129-166. New York: Wiley-Liss.

Crotty, T. L. and Jayne, B. C. (2015). Trade-offs between eating and moving: What happens to the locomotion of slender arboreal snakes when they eat big prey? *Biol. J. Linn. Soc.* **114**, 446-458.

Cundall, D. (1987). Functional morphology. In *Snakes: Ecology and Evolutionary Biology* (ed. R. A. Seigel, J. T. Collins and S. S. Novak), pp. 106-140. New York: McGraw-Hill.

Cundall, D. and Greene, H. W. (2000). Feeding in snakes. In *Feeding: Form, Function and Evolution in Tetrapod Vertebrates* (ed. K. Schwenk), pp. 293-333. New York: Academic Press.

Frolich, L. M. and Biewener, A. A. (1992). Kinematic and electromyographic analysis of the functional role of the body axis during terrestrial and aquatic locomotion in the salamander *Ambystoma tigrinum*. *J. Exp. Biol.* **162**, 107-130.

Gans, C. (1974). *Biomechanics. An Approach to Vertebrate Biology*. Ann Arbor: University of Michigan Press.

Gasc, J. P., Cattaert, D., Chaserat, C. and Clarac, F. (1989). Propulsive action of a snake pushing against a single site: its combined analysis. *J. Morphol.* **201**, 315-329.

Gray, J. (1968). *Animal Locomotion*. London: Weidenfield and Nicolson.

Gray, J. and Lissmann, H. W. (1938). Studies in animal locomotion VII. Locomotory reflexes in the earthworm. *J. Exp. Biol.* **15**, 506-517.

Hildebrand, M. (1976). Analysis of tetrapod gaits: general considerations and symmetrical gaits. In *Neural Control of Locomotion* (ed. R. M. Herman, S. Grillner, P. S. G. Stein and D. G. Stuart), pp. 203-236. New York: Plenum Press.

Jayne, B. C. (1986). Kinematics of terrestrial snake locomotion. *Copeia* **1986**, 915-927.

Jayne, B. C. (1988a). Mechanical behavior of snake skin. *J. Zool.* **214**, 125-140.

Jayne, B. C. (1988b). Muscular mechanisms of snake locomotion: an electromyographic study of lateral undulation of the Florida banded water snake (*Nerodia fasciata*) and the yellow rat snake (*Elaphe obsoleta*). *J. Morphol.* **197**, 159-181.

Jayne, B. C. (1988c). Muscular mechanisms of snake locomotion: an electromyographic study of the sidewinding and concertina modes of *Crotalus cerastes*, *Nerodia fasciata* and *Elaphe obsoleta*. *J. Exp. Biol.* **140**, 1-33.

Jayne, B. C. and Bennett, A. F. (1990). Scaling of speed and endurance in garter snakes: a comparison of cross-sectional and longitudinal allometry. *J. Zool. London* **220**, 257-277.

Jayne, B. C. and Davis, J. D. (1991). Kinematics and performance capacity for the concertina locomotion of a snake (*Coluber constrictor*). *J. Exp. Biol.* **156**, 539-556.

Jorgensen, R. M. and Jayne, B. C. (2017). Three-dimensional trajectories affect the epaxial muscle activity of arboreal snakes crossing gaps. *J. Exp. Biol.* **220**, 3545-3555.

Kier, W. M. and Smith, K. K. (1985). Tongues, tentacles and trunks - the biomechanics of movement in muscular-hydrostats. *Zool. J. Linn. Soc.* **83**, 307-324.

Lissmann, H. W. (1950). Rectilinear locomotion in a snake (*Boa occidentalis*). *J. Exp. Biol.* **26**, 368-379.

Marvi, H., Bridges, J. and Hu, D. L. (2013). Snakes mimic earthworms: propulsion using rectilinear travelling waves. *J. R. Soc. Interface* **10**, 20130188.

Montgomery, G. G. and Rand, A. S. (1978). Movements, body temperature and hunting strategy of a *Boa constrictor*. *Copeia* **1978**, 532-533.

Moon, B. R. and Gans, C. (1998). Kinematics, muscular activity and propulsion in gopher snakes. *J. Exp. Biol.* **201**, 2669-2684.

Mosauer, W. (1932). On the locomotion of snakes. *Science* **76**, 583-585.

Pough, F. H. and Groves, J. D. (1983). Specializations of the body form and food habits of snakes. *Am. Zool.* **23**, 443-454.

Pyron, R. A., Burbrink, F. T. and Wiens, J. J. (2013). A phylogeny and revised classification of Squamata, including 4161 species of lizards and snakes. *BMC Evol. Biol.* **13**, 93.

Quillin, K. J. (1999). Kinematic scaling of locomotion by hydrostatic animals: ontogeny of peristaltic crawling by the earthworm *Lumbricus terrestris*. *J. Exp. Biol.* **202**, 661-674.

Secor, S. M., Jayne, B. C. and Bennett, A. F. (1992). Locomotor performance and energetic cost of sidewinding by the snake *Crotalus cerastes*. *J. Exp. Biol.* **163**, 1-14.

Tytell, E. D., Hsu, C.-Y., Williams, T. L., Cohen, A. H. and Fauci, L. J. (2010). Interactions between internal forces, body stiffness, and fluid environment in a neuromechanical model of lamprey swimming. *P. Natl. Acad. Sci. USA* **107**, 19832-19837.

Walton, M., Jayne, B. C. and Bennett, A. F. (1990). The energetic cost of limbless locomotion. *Science* **249**, 524-527.

Williams, T. L., Grillner, S., Smoljaninov, V. V., Wallen, P., Kashin, S. and Rossignol, S. (1989). Locomotion in lamprey and trout: the relative timing of activation and movement. *J. Exp. Biol.* **143**, 559-566.

Yi, H. and Norell, M. A. (2015). The burrowing origin of modern snakes. *Sci. Adv.* **1**, e1500743.